

Research on a Magnetic Refrigeration Cycle for Hydrogen Liquefaction

T. Utaki¹, K. Kamiya², T. Nakagawa¹, T. A. Yamamoto¹
and T. Numazawa²

¹Graduate school of Engineering, Osaka University
Osaka, 565-0871, Japan

²National Institute for Materials Science
Tsukuba Magnet Laboratory
Tsukuba, Ibaraki, 305-0003, Japan

ABSTRACT

For the upcoming hydrogen society, there are several key technological issues such as hydrogen generation, liquefaction, storage, and transportation. Magnetic refrigeration systems based on the magnetocaloric effect involve intrinsically higher energy efficiency than conventional refrigeration systems at cryogenic temperatures. Thus, they are potentially attractive candidates as a means of hydrogen liquefaction. However, there is little reported data on the refrigeration performance of magnetic refrigeration used as a hydrogen liquefier. To provide the needed data, we have evaluated the system parameters required for the design optimization of magnetic refrigerators and estimated their coefficient of performance using a numerical simulation model.

The magnetic refrigerator model we have constructed is based on a multistage active magnetic regenerative (AMR) cycle. In our current model, an ideal magnetic material with constant magnetocaloric effect is employed as the magnetic working substance. The maximum applied field is 5 T, and the liquid hydrogen production rate is 0.01 t/day. Starting from liquid nitrogen temperature (77 K), it is assumed that four separate stages of refrigeration are needed to cool the hydrogen. The results of the simulation show that the use of a magnetic refrigerator for hydrogen liquefaction is possibly more efficient than the use of conventional liquefaction methods.

There are several candidate arrangements of magnetic refrigeration liquefaction cycles starting from either room temperature (300 K), or from the temperature of liquid natural gas (120 K). We show trial results on efficiency and cooling power for several.

INTRODUCTION

There are several key technological issues such as hydrogen generation, liquefaction, storage and transportation for the upcoming hydrogen energy society. Magnetic refrigeration systems have started to attract attention as a candidate for hydrogen liquefaction. Such systems make use of the magnetocaloric effect (MCE) in which some magnetic materials exhaust or absorb heat with the application and removal of an external magnetic field. Magnetic refrigeration systems are environmentally friendly, have quiet operation, and are possibly more efficient than conventional liquefaction methods.

Kamiya has been developing a Carnot-type magnetic refrigerator (CMR) for hydrogen liquefaction.¹ The magnetic refrigerator operates on the Carnot cycle and liquefies precooled hydrogen at 20 K, absorbing the latent heat. The demonstrated system reached 40% Carnot with a 25 W cooling power at 0.45 Hz; this is equivalent to 5 kg/day of liquid hydrogen.

However, there is little reported on magnetic refrigerators operating between the supplied gaseous hydrogen temperature (300 K) and the CMR hot end temperature (22 K). Therefore, we have constructed a model of a multistage active magnetic regenerative (AMR) cycle to precool hydrogen through this temperature range. In addition, we have evaluated the system parameters required for the design optimization of an active magnetic regenerative refrigerator (AMRR) and estimated its performance using a numerical simulation.

In general, it is helpful to precool hydrogen prior to liquefaction using a cryogenic liquid such as liquid nitrogen (LN₂) or liquid natural gas (LNG). Therefore, we chose three system configurations to analyze with our numerical simulation. In the first case, Figure 1, the supplied hydrogen is precooled by the AMRR only. In this case it is assumed that the magnetic refrigeration system precools the hydrogen from 300 K to 22 K using approximately 7-9 stages of AMRR. In the second case, Fig. 2, the supplied hydrogen is precooled from 300 K to 77 K by LN₂, and from 77 K to 22 K by 3 stages of AMRR. In the third case, Fig. 3, the supplied hydrogen is precooled from 300 K to 120 K by LNG, and from 120 K to 22 K by 5 stages of AMRR.

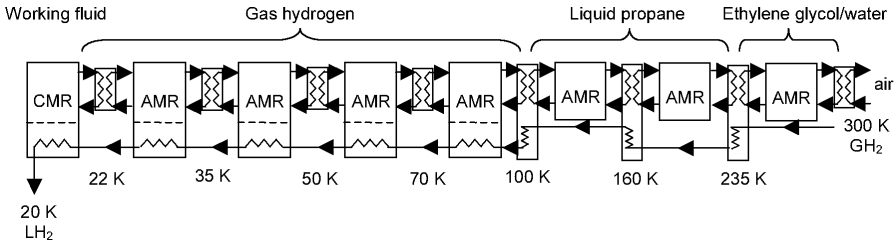


Figure 1. Case 1: magnetic refrigerator for hydrogen liquefaction combines 8-stage AMRR with CMR.

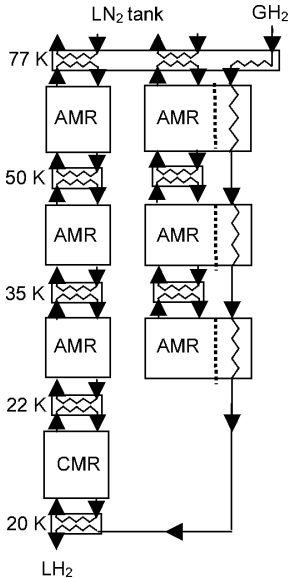


Figure 2. Case 2: magnetic refrigerator for hydrogen liquefaction combines 3-stage AMRR with CMR and precooling by LN₂.

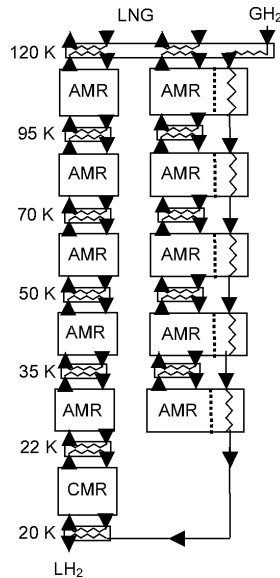


Figure 3. Case 3: magnetic refrigerator for hydrogen liquefaction combines 5-stage AMRR with CMR and precooling by LNG.

Efficiency

We evaluate each stage of the magnetic refrigerator by using the coefficient of performance (COP), which is usually defined as follows:

$$\text{COP} = \frac{Q_c}{W_{\text{in}}} \quad (1)$$

where Q_c is the cooling power, i.e. the heat absorbed from the cold end. W_{in} is the work input into the magnetic refrigerator.

We evaluate the magnetic refrigerator for hydrogen liquefaction using the efficiency, η , defined as follows:

$$\eta = \frac{W_{\text{min}}}{W_{\text{total}}} \times 100 \quad (2)$$

where W_{total} is the total work input for hydrogen liquefaction, and W_{min} is the minimum theoretical work for hydrogen liquefaction. The minimum theoretical work for liquefaction is that required to reversibly remove heat from hydrogen between a defined initial gaseous state and another defined final liquid state. It can be expressed thermodynamically in terms of the availability function which is a point function and is defined as follows:

$$W_{\text{min}} = (H_i - H_f) - T_0 (S_i - S_f) \quad (3)$$

The symbols H and S represent thermodynamic properties of enthalpy and entropy, respectively, while the subscripts, i and f , refer to the initial and final states. T_0 is the hot-end temperature at which heat is rejected to the surroundings.²

SIMULATION MODEL

The simulation model used in this work has been developed by Engelbrecht and improved by joint research between NIMS and the University of Wisconsin.³ It can calculate the temperature profile, COP, and cooling power using one-dimensional energy equations of the working fluid and magnetic regenerator bed.

The AMRR consists of regenerator beds, magnets, pumps, and heat exchangers. The regenerator beds are packed with particle magnetic materials that are subjected to changing magnetic fields controlled by external magnets. The working fluid alternates between the hot end and the cold end synchronously with the external magnetic field changes. By repeating the process, this regenerator operates as a refrigerator and the forms the AMR cycle.

Governing Equations

The one-dimensional energy equations of the working fluid and magnetic regenerator bed were obtained by performing energy balances across differential segments. Subscripts f and r denote the working fluid and regenerator bed, respectively.

The energy balance on the working fluid is:

$$\dot{m}(t) \frac{\partial}{\partial x} [c_f(T_f)T_f] + \frac{Nu(\text{Re}_f, \text{Pr}_f)k_f(T_f)}{d_h} a_s A_c (T_f - T_r) + \rho_f(x) A_c \varepsilon \frac{\partial}{\partial x} [c_f(T_f)T_f] = \left| \frac{\partial p}{\partial x} \frac{\dot{m}(t)}{\rho_f(x)} \right| \quad (4)$$

The first term in Eq. (4) represents the enthalpy change of the flow, the second term represents heat transfer from the fluid to the regenerator, the third term represents the energy stored by the fluid, and the fourth term represents viscous dissipation.

The energy balance on the magnetic material in the regenerator is:

$$\frac{Nu(\text{Re}_f, \text{Pr}_f)k_f(T_f)}{d_h} a_s A_c (T_f - T_r) + A_c (1 - \varepsilon) \mu_0 H \frac{\partial M}{\partial t} - k_{eff} A_c \frac{\partial^2 T_r}{\partial x^2} = \rho_r A_c (1 - \varepsilon) \frac{\partial u_r}{\partial t} \quad (5)$$

The first term in Eq. (5) represents heat transfer from the fluid to the regenerator, the second term represents the magnetic work transfer, the third term is axial conduction, and the fourth term repre-

sents the energy stored by the regenerator. Within the individual terms, $\dot{m}(t)$ is the time variation of the fluid mass flow rate, $\mu_0 H(x, t)$ is the variation of the magnetic field in time and space, and k_{eff} is the effective conductivity of the fluid and regenerator. Fluid properties include the specific heat capacity (c_p), viscosity (μ_p), density (ρ_p) and thermal conductivity (k_p). Regenerator geometry is characterized by a hydraulic diameter (d_h), porosity (ϵ) and specific surface area (a_s). The overall size of the regenerator is specified according to its length (L) and total cross-sectional area (A_c). The Nusselt number (Nu) is assumed to be a function of the local Reynolds number (Re) and Prandtl number (Pr) of the fluid.

Key Assumptions

The following assumptions were made in the derivation and application of the governing equations:

- Density of the working fluid is constant in each regenerator spatial node; therefore the mass flow rate does not vary spatially in the matrix and the mass of the fluid entrained in the matrix is constant. The density is evaluated at the local average temperature of the fluid at each spatial step
- Axial conduction is ignored in the fluid and instead is applied to the matrix and modeled using the concept of effective bed conductivity.
- The magnetization and demagnetization processes are assumed to be internally reversible.
- Thermal capacity of the fluid is lumped together with that of the regenerator; this simplifies the governing equations and stabilizes the numerical solution considerably.
- The Ergun equation is used to predict pressure drop in the regenerator packed with a particle magnetic material.⁴

Model Input

The parameters used to perform this work are shown in Table 1. Hydrogen gas is supplied at 300 K and precooled to the CMR hot end temperature (22 K) by the multi-staged AMRR. As the hydrogen is assumed to be first precooled by a cryogenic liquid (LN₂ or LNG), the AMRR operates from 77 K or 120 K to 22 K. The liquid hydrogen production rate is 0.01 t/day. We can calculate by Eq. (3) that the minimum theoretical work for this production rate is 1.65 kW. The maximum applied field is 5 T, the number of the refrigerator beds in the AMRR is six, and one cycle period is 0.2 sec. The sphere size of the packing is 0.2 mm. Different working fluids were chosen depending on the operating temperature range. As shown in Table 2, hydrogen, liquid propane, and ethylene glycol/water were applied as the working fluids. In our current model, an ideal magnetic material with constant magnetocaloric effect is employed as the magnetic working substance.

Table 1. Parameters used in this work.

Parameter	Value	Parameter	Value
heat rejection temperature	300 K	number of beds	6
load temperature	22 K	period	0.2 sec (5 Hz)
Production rate	0.01 t/day	sphere size for packing	0.2 mm
maximum applied field	5 Tesla	Working fluid	varies

Table 2. Working fluid and temperature range used in each stage in case 1.

Stage	Temperature range [K]	Working fluid	Stage	Temperature range [K]	Working fluid
1	22-35	hydrogen	5	100 - 144.3	propane
2	35-50	hydrogen	6	144.3 - 188.6	propane
3	50-70	hydrogen	7	188.6 - 233	propane
4	70-100	hydrogen	8	233 - 300	ethylene glycol/water

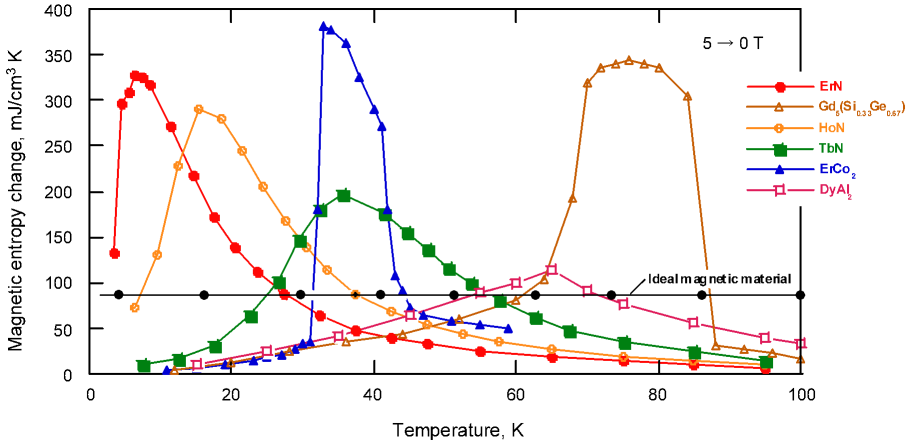


Figure 4. Magnetic entropy change of an ideal magnetic material used in this simulation.

Magnetic Material

In order to simulate an ideally layered regenerator, an artificial magnetic material was synthesized using 0 Tesla properties of $Gd_{0.96}Er_{0.04}$. The entropy at other magnetic fields was calculated by adding the maximum change in entropy with magnetization for each magnetic field to the 0 Tesla entropy. Figure 4 shows the magnetic entropy change induced by demagnetization from 5 to 0 T for some excellent magnetic materials in this temperature range. Also shown is the assumed magnetic entropy change of our ideal magnetic material; it is constant at $86.2 \text{ mJ/cm}^3 \text{ K}$, independent of temperature.

Ortho-Para Conversion

One must also take into account the heat of ortho-hydrogen to para-hydrogen conversion when liquefying hydrogen. The heat of conversion, which amounts to 703 J/g at the normal boiling point, is substantial and exceeds the latent heat of condensation, which amounts to only 444 J/g . If the unconverted liquid hydrogen is placed in a tank, the heat of conversion will be released in the form of increased evaporation. Therefore, one needs to convert ortho-hydrogen to para-hydrogen with a catalyst during the liquefaction process.²

The conversion of ortho-hydrogen to para-hydrogen is assumed to take place instantaneously, assuming perfect catalysis in the regenerator bed. In this limit, the conversion from ortho-hydrogen to para-hydrogen acts like an additional heat capacity of the fluid. The modified specific heat of hydrogen is calculated using the formula below.

$$c_{mod}(T_f) = c(T_f) + \frac{\Delta E_{120-30 \text{ K}}}{90 \text{ K}} \tag{6}$$

where $\Delta E_{120-30 \text{ K}}$ is the energy associated with the conversion of ortho to para between 120 K and 30 K from Timmerhaus and Flynn⁵, c_{mod} is the specific heat modified to correct for ortho-hydrogen to para-hydrogen conversion, and T_f is the fluid temperature. The calculated correction factor is 5110.0 J/kg-K .

RESULTS AND DISCUSSION

Optimization Technique

Magnetic refrigerators essentially have a variable cooling power which is dependent on the volume of the regenerator, the bed length to cross sectional area aspect ratio, and the working fluid mass flow rate. Therefore, we have evaluated the system parameters versus the volume of the regenerator, aspect ratio, and the working fluid mass flow rate as required to optimize the AMRR design.

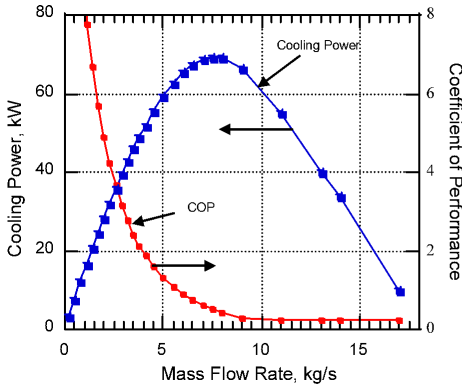


Figure 5. Cooling power and COP of a magnetic refrigerator with a fixed regenerator volume and aspect ratio as a function of the fluid mass flow rate.

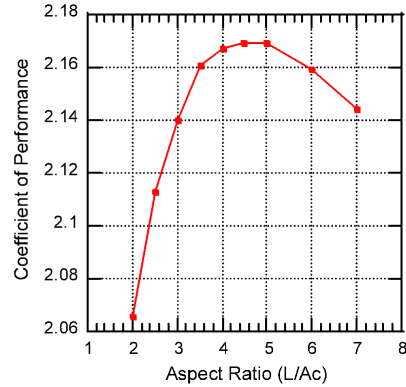


Figure 6. COP of a magnetic refrigerator as a function of the aspect ratio.

Mass Flow Rate. For a regenerator of a fixed length and cross-sectional area, the functional dependence of the cooling power as a function of working fluid mass flow rate may be determined. Figure 5 illustrates the cooling power and COP for an AMRR using the parameters listed in Table 1 and a regenerator of a fixed volume (15 L) and aspect ratio ($L/d=4$). The AMRR operating temperature range is 240 to 230 K, and the working fluid is propane. Notice that it is possible to produce a specified cooling power using one of two possible mass flow rates. In the figure, the lower mass flow rate always corresponds to a higher COP. In order to design a bed for a given cooling power (50 kW in this case), the lowest mass flow rate that is able to achieve the higher COP is selected.

Aspect Ratio. Figure 6 illustrates COP as a function of aspect ratio for a 20 L regenerator bed producing 5.3 kW of cooling power. The AMRR operating temperature range is 240 to 185 K, and the working fluid is propane. Figure 6 shows that there exists an optimal aspect ratio where the COP is maximized; lower aspect ratios result in excessive conduction losses, and higher aspect ratios result in excessive pumping losses.

Regenerator Volume. Figure 7 illustrates COP as a function of regenerator volume. This curve was generated using a cooling power of 0.1 kW and the optimal aspect ratio for each volume. The AMRR operating temperature range is 35 to 22 K, and the working fluid is hydrogen. Figure 7 shows that the COP of an AMR depends on the volume of the regenerator bed used. As the AMR regenerator volume increases, the operating efficiency also increases. Of course, larger regenerator volumes are also associated with higher initial investments, and therefore there must be an economically optimum regenerator volume.

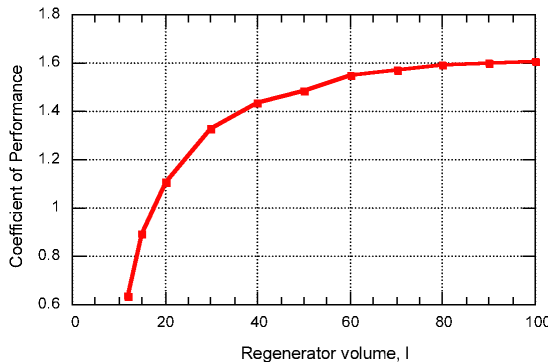


Figure 7. COP of a magnetic refrigerator producing 0.1 kW of cooling power at its optimal aspect ratio.

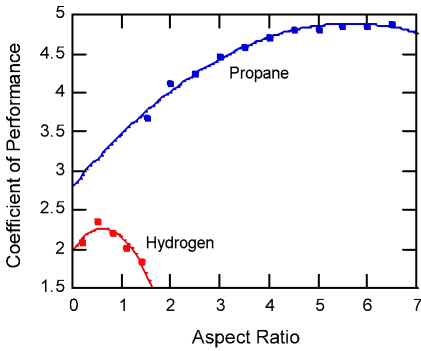


Figure 8. Comparison of propane and hydrogen as the working fluid.

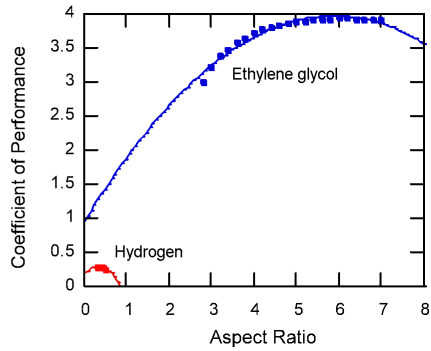


Figure 9. Comparison of ethylene glycol/water and hydrogen as the working fluid.

This optimization technique is used to choose the combination of the optimum mass flow rate and aspect ratio of an AMRR of specified regenerator volume and cooling power for various applications.

Working Fluid

We selected ethylene glycol/water as the working fluid for the temperature range between 300 K and 235 K, liquid propane for the temperature range between 235 K and 95 K, and hydrogen for the temperature range between 95 K and 22 K. Propane is a liquid between approximately 260 K and 90 K at a pressure of 3 atm. Ethylene glycol/water is a mixture with a concentration of 56 % ethylene glycol and has a freezing point of 228.3 K and a boiling point well above 300 K.

In order to compare the performance of a refrigerator using hydrogen as a working fluid with one using propane, a short analysis was performed. The results are shown in Figure 8. The COP of each refrigerator was calculated for an AMR producing 100 W of cooling power with a regenerator volume of 2 L. The temperature range was 110 to 100 K. The aspect ratio is defined as the ratio of the bed length to cross-sectional area. Figure 8 shows that propane clearly outperforms hydrogen as a working fluid. With a well designed heat exchanger, it will be more efficient to use a heat exchanger between the propane and hydrogen than to directly cool the hydrogen by using it as the working fluid.

Similarly, Figure 9 shows results comparing the performance of a refrigerator using hydrogen as a working fluid to one using ethylene glycol/water. The COP of each refrigerator was calculated for an AMR producing 350 W of cooling power. The temperature range was 265 to 245 K. The regenerator volume with ethylene glycol/water is smaller than that required with hydrogen. Similar to propane, the performance of a refrigerator using a mixture of ethylene glycol and water is significantly higher than one using hydrogen or gaseous propane as the working fluid.

Overall Performance

The operating conditions and performance of the overall system in case 2 are given in Table 3. The system is a 3-stage AMRR that cools hydrogen from 77 K to 22 K (CMR hot end temperature) assuming the hydrogen has been precooled using LN₂. In Table 3, Q_{H2} is the power needed to cool

Table 3. Results for Overall System Performance of AMRR in Case 2.

Stage	Temperature range [K]	Q _{H2} [W]	Q _{lower} [W]	Q _{ref} [W]	COP	Q _{rej} [W]	W _{in} [W]
1	22-35	26.4	0.0	26.4	0.6964	64.4	37.9
2	35-50	45.0	64.4	109.3	1.0320	215.3	105.9
3	50-77	76.6	215.3	291.9	0.5051	869.8	577.9
							721.8

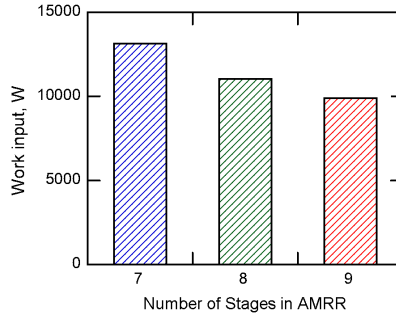


Figure 10. Comparison of the total work input versus number of stages in case-1 AMRR.

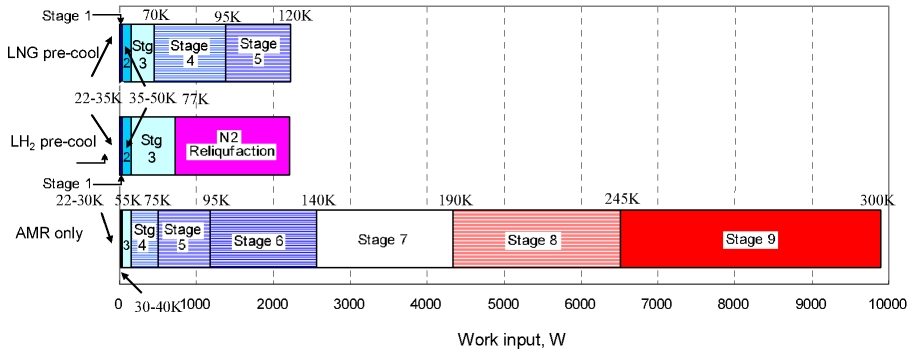


Figure 11. Comparison of the total work input for 9-stage AMRR, 3-stage AMRR + LN₂ precooling, and 5-stage AMRR + LNG precooling.

the hydrogen from the hot end to the cold end temperature for each stage, Q_{lower} is the rejection from the lower temperature cooling stage, Q_{ref} is the total cooling power of each stage, Q_{rej} is the heat rejection at the hot end for each cooler, and W_{in} is the work input. The total work input to this system is 0.72 kW. In addition, for the case pre-cooled by LN₂, one needs to add the work input for N₂ reliquefaction to obtain the total work input to the system. In this study, we assumed that the work input for N₂ reliquefaction was approximately 1.49 kW.

Work Input

For the 7 to 9-stage AMRR (case 1) the total work input was determined to be 13.09 kW, 11.08 kW, and 9.90 kW, respectively. Similarly, for the 5-stage AMRR in case 3 the total work input was 2.23 kW. Figure 10 shows a comparison of the total work input for the 7 to 9-stage AMRR. As the number of stages in the AMRR increases, the work input decreases. Of course, a larger number of stages is also associated with higher initial investments, and therefore there must be an economically optimum number of stages.

Figure 11 shows a comparison of the total work input for a 9-stage AMRR, a 3-stage AMRR plus LN₂ precooling, and a 5-stage AMRR plus LNG precooling. The total work input for the 9-stage AMRR, 3-stage AMRR plus LN₂ precooling, and 5-stage AMRR plus LNG precooling is 9.90 kW, 2.21 kW, and 2.23 kW, respectively. The most efficient is the 3-stage AMRR plus LN₂ precooling.

Liquefaction Efficiency

We evaluated the liquefaction efficiency of the magnetic refrigeration systems in case 2 using Eq. (2). The total work input is the work input for the 3-stage AMRR plus LN₂ precooling, the input power to the CMR, and the power to a 3-stage AMRR to cool the exhaust heat from the CMR. We

assumed that the %Carnot efficiency of the CMR is 50 %. Therefore, the power input for the CMR is 0.01 kW. The power input for the 3-stage AMRR to cool the exhaust heat from the CMR was determined from numerical simulation to be 1.30 kW. Summing these contributors gives a total work input for hydrogen liquefaction of 3.52 kW.

We now define liquefaction efficiency as the ratio of the minimum work, 1.65 kW, to the total work input, 3.52 kW. The liquefaction efficiency of the magnetic refrigerator for hydrogen liquefaction is 46.9%.

CONCLUSIONS AND SUMMARY

We have studied a variety of magnetic refrigeration system configurations for hydrogen liquefaction and evaluated their system parameters and work input by numerical simulation. The best performance was achieved by a combined CMR plus a 3-stage AMRR with LN_2 precooling. It had a total work input of 3.52 kW and had a liquefaction efficiency of 46.9 %. This provides promise that magnetic refrigeration systems may be able to achieve higher efficiency than conventional liquefaction methods.

ACKNOWLEDGMENT

Financial support of this collaborative work with The Institute of Applied Energy was provided by NEDO project WE-NET TASK 12, Search and Research of Innovative and Leading Technologies. It is greatly appreciated.

REFERENCES

1. Kamiya, K., "Design and Build of Magnetic Refrigerator for Hydrogen Liquefaction," *Adv. in Cryogenic Engineering*, Vol. 51, Amer. Institute of Physics, Melville, NY (2006), pp. 591-597.
2. Baker, C. B., "A Study of the Efficiency of Hydrogen Liquefaction," *International Journal of Hydrogen Energy*, Vol.3, (1978), pp. 321-334.
3. Engelbrecht, K. L., "A Numerical Model of an Active Magnetic Regenerator Refrigeration System," *Master thesis*, University of Wisconsin, (2004).
4. Ergun, S., "Fluid flow through packed columns," *Chemical Engineering Progress*, Vol. 48, No. 2, (1952), pp. 89-94.
5. Timmerhaus, K. D., *Cryogenic Process Engineering*, Plenum Publishing Corporation, New York (1989).